Quasi-Gaussian velocity distribution of a vibrated granular bilayer system

Alexis Burdeau and Pascal Viot
Laboratoire de Physique Théorique de la Matière Condensée, Université Pierre et Marie Curie, 4 Place Jussieu, 75252 Paris Cedex 05, France

(Received 1 September 2008; revised manuscript received 3 April 2009; published 19 June 2009)

We investigate using a discrete element method the kinetic properties of a system composed of a bilayer of granular spheres submitted to a vertical vibration. For moderate dimensionless acceleration, no mixing between layers is observed and the horizontal velocity distributions of the top-layer particles with are quasi-Gaussian. The robustness of this phenomenon is examined for a variety of physical parameters (acceleration of the bottom plate, mass ratio, layer coverage, etc.). A microscopic analysis of the simulation dynamics leads to a simple picture of the underlying mechanisms.

DOI: 10.1103/PhysRevE.79.061306 PACS number(s): 45.70.Qj, 89.75.Kd

I. INTRODUCTION

Granular particle dynamics are dominated by dissipation due to the inelastic collisions occurring between particles. In order to maintain granular systems in a steady state, it is necessary to provide kinetic energy continuously. In many experiments, energy injection is provided at the boundaries of the system: in dimension 3, inhomogeneities in temperature and/or density gradient are present, leading, for instance, to convection [1] and pattern formation [2]. To minimize these effects, it is tempting to consider two-dimensional (2D) systems where a vibrating bottom plate supplies energy by a sinusoidal vibration. However, even in the simplest case of granular monolayers, a large variety of patterns occurs [3]: for small dimensionless acceleration, heterogeneities are present and a two-phase coexistence [4] was observed, as well as clustering [5] or melting [6]. At high density, monolayer systems display glassy dynamics with for instance a stretched intermediate scattering function [7,8]. When the acceleration of the vibrating base is increased, the system becomes spatially homogeneous and the velocity distribution displays less deviations from Gaussian. Thus, the way energy is injected into these systems is of crucial importance for their thermostatistic properties.

Recent experiments have attempted to control the mechanism of energy injection in quasi-2D vibrated systems. They have revealed that nonequilibrium steady states (NESS) can display features surprisingly close to those observed in equilibrium systems: Prevost *et al.* [9] investigated a monolayer of steel beads on a base-plate subject to a sinusoidal displacement in the vertical direction. The dimensionless acceleration of the vibrating plate is denoted $\Gamma = A(2\pi f)^2/g$, where g is the gravity, A is the amplitude of the oscillations, and f is the frequency. When $\Gamma \geq 1.5$, the plate is rough and the density is low, the velocity distribution is very similar to a Gaussian. In their recent work, Reis *et al.* [10] claimed to observe characteristic features of the stochastic thermostat [11] on the velocity distribution of a vibrated granular monolayer. Baxter and Olafsen [12] experimentally studied a vibrated bilayer system, where the bottom layer was dense and composed of dimer beads and the top layer was composed of plastic beads. The base of the cell, a horizontal circular plate, was vibrated sinusoidally in the vertical direction. The excitation was tuned from $\Gamma = 1.75$ to 2.25 such that the layers were stable. As the density parameter, the coverage of the top-layer c was defined as the ratio of the number of particles in the layer divided by the number of particles there would be in a closed packed configuration: naming η the packing fraction, $c = \eta/\eta_{\max}$. It was varied from $c = 0.2$ to $c = 0.8$. The horizontal velocities of the light particles (second layer) were monitored to build the velocity distribution function. Deviations from Gaussian were quantified by the kurtosis $F = \frac{\langle v^4 \rangle}{\langle v^2 \rangle^2}$, which is equal to 3 for a Gaussian distribution. The experimental results showed that the horizontal velocity distributions of the top layer were very close to Gaussian, ($|F-3| \leq 0.05$), within the parameters range presented above (acceleration, density, and particle size). Conversely, the horizontal velocity distribution of the heavy-particle layer, as well as the vertical velocity distributions remained strongly non-Gaussian ($|F-3| \geq 1$).

The purpose of this paper is twofold: first to build a simple but realistic model which captures the observed features in the experiment of Baxter and Olafsen [12]; second, to understand how the energy injection provided by the first-layer particles can lead to quasi-Gaussian velocity distributions for the top-layer particles. With this objective, we analyze several microscopic quantities to get insight into the role of the first layer. We also examine in detail the robustness of this behavior by varying microscopic parameters of the system. In addition we consider the situation where the particles of the first layer are glued to the vibrating plate, mimicking Prevost's experiment [9].

II. MODEL

For the sake of simplicity, we have used simple spheres instead of the flexible dumbbells used in experiments [12] for the first layer. As the density of the first layer is very high, we expect that the details of the interactions among particles of the first layer are not relevant, except for preventing the penetration of light particles of the second layer into interstitial regions, which may occur when the system is submitted to vibrations. Our simulation model thus consists of a number N_1 of heavy spherical particles placed at the bottom of the simulation cell and N_2 light spherical particles forming the second layer. The parameters have been chosen as close

 ©2009 The American Physical Society

as possible to the experimental system. The mass of the light particles is $M=22.9$ mg, and the mass of the heavy spheres is taken as one half of the mass of the real dimers, namely, $m=92.5$ mg for the monomers. The diameters of light and heavy particles are the same and equal to 3 mm, as in the experiment. Periodic boundary conditions are used in the horizontal directions. We checked that the role of the boundary conditions is negligible for the properties of the steady state by varying the size of the simulation cell. In this study, the simulations were carried out on a system with 2500 spheres in the first layer. These spheres were initially placed on a triangular lattice, with the packing fraction of the first layer equal to $\eta=0.9$ (or $c=1$).

The collisions between spheres, as well as the collisions between spheres and the vibrating bottom, are inelastic. In addition to collisions, the particles are subject to a constant acceleration due to the (vertical) gravitational field. The viscoelastic forces are modeled by the spring-dashpot model [13] which we briefly introduce now. Let ξ be the virtual overlap between two spherical particles. The simplest force along the line joining the two centers that takes dissipation into account is a damped harmonic oscillator defined as

$$F_n = -k_n\xi - \gamma_n\dot{\xi}, \tag{1}$$

where k_n is related to the stiffness of the material and γ_n is related to the dissipation. This force model allows one to very easily tune certain quantities in the simulation, especially the normal coefficient of restitution e_n, which is constant for all collisions at all velocities in our system. Relevant values of e_n and t_n determine the values of k_n and γ_n, independently of the velocities. The choice of the collision-duration t_n, naturally introduces a microscopic characteristic time. The simulation time step is chosen as $\Delta t=10^{-5}$ s and the mean duration of a collision as $t_n=10^{-3}$ s. We have verified that $\Delta t=t_n/100$ gives accurate results.

In addition, we introduce a frictional force by taking the tangential component of the force as $F_t=-\min(|k_t\zeta|,|\mu F_n|)$, where k_t is related to the tangential elasticity and ζ is the tangential displacement since the contact was first established. We used a ratio $k_t/k_n=2/7$ with $\mu=0.25$.

III. SIMULATION RESULTS

By choosing the normal coefficient e_{n_i} for the different types of collisions, the normal force is then well defined. The force model described above and the experimental setup lead us to select five values of e_{n_i} corresponding to the different types of collision i in the system. We ran simulations for various values of e_{n_i} from 0.4 to 0.8 (see Fig. 1). For these values the deviations of the velocity distributions from Gaussian are small, but the granular temperature, defined as $T=\frac{1}{2}M\langle v^2\rangle$ (where v is velocity in the xy plane), varies by a factor 3.

The best agreement of the observed T with a deviation compatible with experiments is obtained for $e_n=0.5$ for the particles of the first layer, and we chose $e_n=0.7$ for the other types of collisions. The value $e_n=0.5$ for the collisions within the first layer corresponds to strongly dissipative collisions,

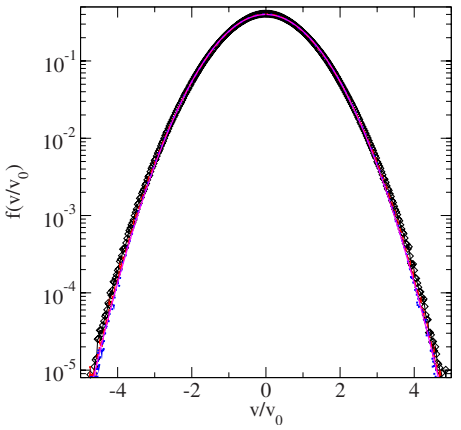

FIG. 1. (Color online) Normalized velocity distributions of the light particles for different values of $e_n=0.5,0.6,0.7$ (for any type of collision) at $\Gamma=2$ and $c=0.2$, corresponding respectively to diamonds (black) and the dashed (red) and dotted (blue) curves. The magenta solid curve is a Gaussian fit. The normalizing factor is the root mean-squared velocity $v_0=\sqrt{\langle v^2\rangle}$.

but the first layer of our system is composed of monomers instead of the dimers used in the experiment. We assume that the dissipation occurring in a layer of composite dimers is much more significant than in a layer of simple spheres. The planar-temperature T decreases with increasing frequency and with increasing coverage, as observed experimentally. This result is related to the decrease in the amplitude of the excitation in the first case, the light spheres being more likely to sit on the lattice of the first layer, and to the increase in the number of collisions in the second case.

Simulations were performed by increasing the coverage of the top layer, namely, increasing the number of the light particles, all others parameters being unchanged ($\Gamma=2$, e_n, m, and M). This is illustrated in Fig. 2 which shows the variation in the kurtosis of the light-particles velocity distribution with the coverage. Note that when the coverage of the top layer goes to zero, the flatness of the velocity distribution approaches a value slightly below 3, which is due to the existence of residual velocity correlations in the tracer limit.

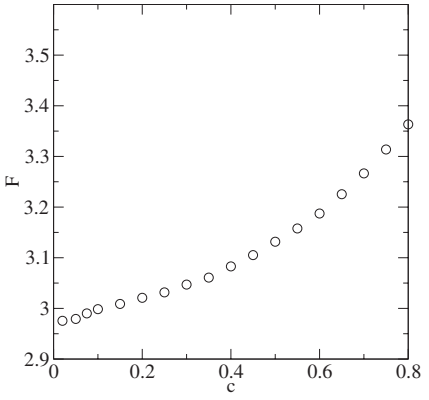

FIG. 2. Kurtosis of the light-particles velocity distribution as a function of the coverage c of the top layer, other parameters being constant, $\Gamma=2$ and $f=50$ Hz. The Gaussian character holds for moderate densities.

At high coverage, the deviations from Gaussian become more significant. The remainder of our study is restricted to coverages $c \leq 0.4$.

It is worth noting that with the physical parameters, ($\Gamma = 2$ and $c \leq 0.4$), the kurtosis of the heavy particles in the first layer is always significantly higher than that of the light particles, i.e., $|F-3| \geq 1$, whereas the values of the second layer are very close to Gaussian ones, with $|F-3| \leq 0.1$.

We have studied the influence of the mass ratio M/m of the two species on the velocity distributions in the range [0.1,1]: when the mass of the light particles increases, the kurtosis of the velocity distribution of the light particles increases too. When the mass ratio exceeds 1/3, the kurtosis becomes significantly larger than 3. Deviations from Gaussian are observed even at low coverage: indeed, when the light particles have a mass comparable to that of the heavy particles, they have a non-negligible influence on the bottom-layer dynamics. Due to this feedback effect, strong deviations from Gaussian are observed even in the tracer limit. As our interest is in velocity distributions as close as possible to Gaussian, we do not pursue our investigation for higher coverages.

In summary, our simulation model captures the main characteristics of the velocity distribution for different values of the coefficient of restitution, as well as for different densities of the light particles. The rest of our study concerns both the robustness of the phenomena with respect to the values of the microscopic parameters and the origin of the minimization of velocity correlations.

We first focus on situations where the dimensionless acceleration is varied: an upper bound occurs at $\Gamma = 2.3$, where the excitation is sufficient for ejecting particles of the first layer. When such events occur, an irreversible mixing between layers is observed. Conversely, when decreasing Γ, the flatness of velocity distribution displays small variations and suddenly increases when the excitation becomes too small ($\Gamma \simeq 1.35$) (see Fig. 3). For light particles, the roughness of the first layer is a key ingredient for obtaining a velocity distribution close to a Gaussian profile. To measure its influence, we considered two other systems. We studied the same system, but with top particles 1.5 larger than previous (i.e., $d = 4.5$ mm), keeping the particle mass constant. This corresponds to a system with lower roughness. We also examined the case of glued particles for the first layer (reproducing the experimental setup used in Ref. [9].

As shown in Fig. 3, the kurtosis is always significantly higher in the first case, indicating that in this case the randomization due to the bottom particles is not sufficient. When the particles of the first layer are glued to the vibrating plate, the kurtosis diverges at an acceleration $\Gamma = 1.35$, and decreases monotonously with Γ reaching a plateau at $\Gamma = 1.9$. This shows that the surface roughness must be combined with a "random" local movement of the heavy particles in order to have a velocity distribution whose kurtosis is very close to 3. Although the surface roughness of the first layer randomizes the direction of the postcollisional velocity of the light particles, this mechanism alone is not sufficient to lead to a very good Gaussian velocity profile. When the heavy particles are allowed to move, the magnitude of the light-particle velocity is modified randomly during a collision. Combining these two mechanisms eventually allows one to obtain the "best" profile.

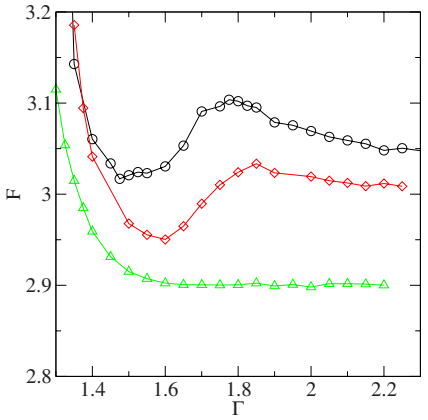

FIG. 3. (Color online) Kurtosis of the light-particles velocity distribution as a function of the dimensionless acceleration for coverage of the top-layer $c = 0.2$. Diamonds and triangles correspond to the system with free and glued bottom particles, respectively. Circles correspond to the system with top particles of diameter $d = 4.5$ mm but with the same mass, the bottom particles being mobile.

The mobility of the light particles has been monitored through the evolution of the coefficient of diffusion as a function of Γ. Close to the smallest acceleration, the coefficient of diffusion goes to zero, which corresponds to the fact that light particles remain trapped in valleys of the rough surface. For higher acceleration, the diffusion coefficient evolves almost linearly (at low coverage): indeed, as illustrated in Fig. 4, at low coverage, the light particles collide more frequently with the first layer than among themselves; the collision frequency is given by the frequency of the vibrating plate. Between two collisions, the particles hop on the surface and the mean-square displacement is roughly given by v^2/f, where v^2 is the mean-square horizontal velocity; this latter quantity being proportional to the dimension-

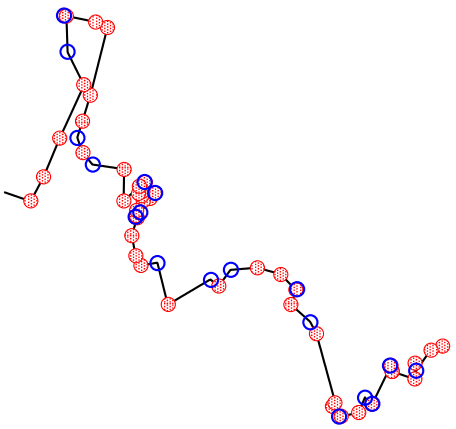

FIG. 4. (Color online) Trajectory of a particle of the top layer: collisions with bottom particles and other top particles are displayed in filled (red) and empty (blue) circles, respectively. Blue collisions are on average separated by several red ones. This randomizing process explains the nearly Gaussian character of the top-layer velocity distribution.

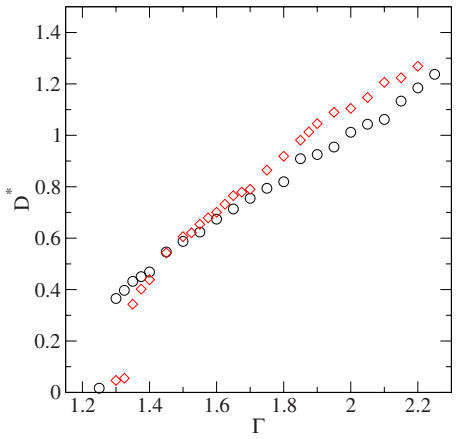

FIG. 5. (Color online) Dimensionless diffusion coefficient, $D^*=D/(fd^2)$, of the light particles as a function of the dimensionless acceleration for a coverage of the top-layer $c=0.2$. Circles and diamonds correspond respectively to the system with free and glued bottom particles.

less acceleration, one obtains a linear relation between the diffusion coefficient and the acceleration (at a given frequency). Similar behavior is obtained for larger top particles and when the first particles are glued on the surface (see Fig. 5).

To verify the homogeneity of the top layer, we have monitored the longitudinal and transverse velocity-correlation functions [9], $C_{\parallel,\perp}(r)=\Sigma_{i\neq j}v_i^{\parallel,\perp}v_j^{\parallel,\perp}/N_r$. Our results are very similar to those obtained experimentally with the same system [14] and indicate the absence of spatial correlations for the velocities of the light particles and the presence of molecular chaos. It can be noted that our simulations agree accurately with the experimental results given in [9], where bottom particles are glued. This reveals that a rough surface is a sufficient ingredient to kill spatial correlations, whereas the mobility of the bottom layer is not crucial. Results are shown in Fig. 6 for $c=0.2$: spatial correlations decrease exponentially on a typical distance which is always less than or

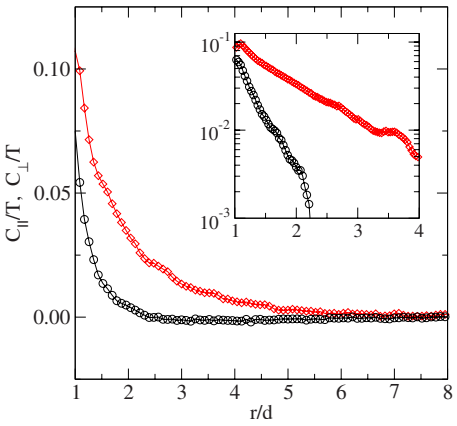

FIG. 6. (Color online) Longitudinal (diamonds) and transverse (circles) velocity correlations as functions of the distance r normalized by the particle diameter d, at coverage $c=0.2$. A fit of the form $C_{\parallel/\perp}\propto e^{-r/r_0}$ gives $r_0=1.1d$ for $C_\parallel$ and $r_0=0.33d$ for $C_\perp$. A semi-log plot of the curves is shown in inset.

comparable to a particle diameter: this ensures the absence of heterogeneity of the granular temperature in the system.

In addition, a very high packing in the bottom layer is also a key ingredient for ensuring homogeneity of the top layer: in a recent paper, Combs *et al.* [15] showed that if the packing fraction of the first layer is decreased, holes appear which rapidly alter the Gaussian character of the velocity distribution. Indeed, light particles become trapped and the system loses homogeneity. In the experimental setup, the packing fraction of the first layer is high, which prevents the appearance of defects in this first layer.

We also studied the velocity correlations in time: the velocity autocorrelation function is not here a relevant quantity, because it is a fast-decaying function and one cannot use it to analyze in detail the influence of the thermostating effect of the first-layer particles on the top-layer particles. We consider here a more appropriate quantity based on the collision statistics: the probability distribution of the scalar product of the pre and postcollisional velocities of a given particle. It is a measure of the correlations appearing between velocities during a collision. It should be noted that this quantity is different from the velocity correlation function as it depends on events and not on time. It can be written formally as

$$P(z)=\langle\delta(z-\mathbf{v}\cdot:\mathbf{v}^*)\rangle, \tag{2}$$

where $\mathbf{v}$ and $\mathbf{v}^*$ are the velocities of a particle before and after a collision, and the brackets correspond to the statistical average on particles.

This quantity is sensitive to the bath velocity distribution and the collision rule and it decays more slowly than the velocity distribution. In addition, for a homogeneous system, if the restitution coefficients are independent of the velocity, and if the dynamics can be described by a Boltzmann equation (Molecular Chaos assumption), an analytical expression of this quantity can be obtained [16]. Assuming that the particle velocity distribution is Gaussian, and for hard inelastic frictionless particles characterized by a constant normal coefficient of restitution e_n, $P(z)$ has a universal feature in the sense that, for $z<0$, $P(z)$ is an exponential in any dimension and its explicit expression is given as a function of physical parameters, i.e., for collisions between particles of mass M,

$$P(z)=P(0)\exp\left(\frac{2}{1+e_n^2}\sqrt{2(1+e_n^2)}+1-e_n\frac{Mz}{T}\right). \tag{3}$$

This distribution reveals to what extent precollisional and postcollisional velocities are correlated through the collision process. By sampling separately the two types of collisions undergone by the light particles, we can evaluate and compare their characteristics. Figure 7 displays the two distributions $P_{lh}(z)$ and $P_{ll}(z)$ corresponding to the horizontal velocities. The subscripts lh and ll denote the collisions between heavy and light particles and those between light particles, respectively. $P_{lh}(z)$ would be a simple exponential distribution (strictly speaking) if the light particles were reflected by a flat surface but due to the randomizing effect of the bottom layer, it is very similar to $P_{ll}(z)$. This clearly indicates the similarity of the collision processes among the light particles and between light and heavy particles: in the horizontal

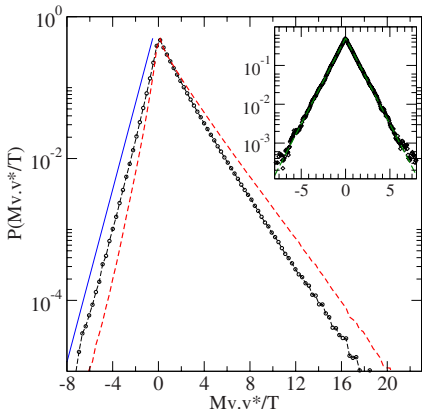

FIG. 7. (Color online) First-collision horizontal velocity distributions $P(z)$ with $z=M\mathbf{v}\cdot\mathbf{v}^*/T$. The dotted (black) and dashed (red) curves correspond respectively to collisions between light particles and between heavy and light particles. The solid (blue) curve corresponds to the exponential decay predicted by Eq. (3) (shifted to the left for clarity) for the dotted curve. The inset displays the tenth-collision velocity distribution as well as the predicted $P_\infty(z)$ (indistinguishable).

plane, the bottom layer behaves as a nearly Gaussian bath in contact with the light-particles population, whereas the heavy particles' velocity distribution is far from being Gaussian. We applied Eq. (3) to the collisions between light particles, with e_n corresponding to the simulation value. The result is displayed for $z<0$ in Fig. 7, showing a very good agreement with the simulation result.

More generally, one can define the nth-collision velocity distribution $P_n(z)$, as the distribution of the scalar product between the precollisional velocity and the postcollisional velocity obtained after n collisions [16]. When n increases, the correlations between the two velocities decrease rapidly and the distribution becomes more and more symmetric. Assuming that the velocity distribution is Gaussian, $P_\infty(z)$ is known analytically: $P_\infty(z)=M\exp(-|z|M/T)/2T$, where T is the granular temperature of the particles. We have also plotted in the inset of Fig. 7 $P_{10}(z)$ for the light particles. The exact result for $P_\infty(z)$ agrees very well with the simulation data for $P_{10}(z)$ except in the tail of the distributions. This shows that the velocity correlations are fully suppressed after few collisions (of any type). Note that the exponential decay is associated with the existence of a quasi-Gaussian velocity distribution.

IV. CONCLUSION

We have presented a simple simulation model, whose results are in very good agreement with the experimental findings of Baxter and Olafsen [12]. We have obtained strong evidence that several ingredients are necessary in order to obtain quasi-Gaussian horizontal velocity distribution for the particles of the top layer: first, the acceleration of the bottom plate must be sufficient for avoiding temperature heterogeneities in the system. Second, the mass ratio between light particles in the top layer and heavy particles in the bottom layer must be less than one third. If not, the velocity distribution of the light particles deviates progressively from Gaussian, even in the tracer limit. Third, the particles of the two layers must be of comparable sizes, so that the first layer appears as a rough surface for light particles and randomizes the direction of the velocity of the light particles during a collision with the bottom layer. Lastly, a rough surface (made of glued particles) is less efficient than a bottom layer of moving particles. We interpret this last characteristic as follows: during interspecies collisions, the amplitude of the velocities of the light particles are changed more "randomly" than in the case of a glued first layer.

In addition, the analysis of the collision statistics confirms that the correlations in the velocities after collisions are well described by the assumption of molecular chaos (Boltzmann equation).

In granular systems, the dissipation during collisions leads in general to strong deviations from Gaussian for the velocity distributions. We have shown here that the bilayer system minimizes these deviations and provides a well controlled system for testing theoretical predictions obtained in the framework of kinetic theories of homogeneous systems. To list a few of these predictions, rotational and translational granular temperatures are expected to be different for anisotropic particles [17] and have been obtained within the assumption of a Gaussian bath. Recent theoretical studies have predicted the possibility of Brownian ratchets [18] or granular rotors [19] whose mechanism is connected to the existence of dissipative collisions; however, the effect depends on the precise shape of the velocity distribution of the bath particles [18]. The bilayer system provides therefore a reference system for investigating quantitatively these phenomena. These examples underline the potential interest of performing a more extensive experimental exploration of this system.

ACKNOWLEDGMENTS

We would like to thank G. W. Baxter and J. S. Olafsen for fruitful discussions and for sharing with us their experimental data, as well as J. Talbot and R. Hawkins for insightful suggestions.

[1] R. D. Wildman, J. M. Huntley, and D. J. Parker, Phys. Rev. Lett. **86**, 3304 (2001).
[2] I. S. Aranson and L. S. Tsimring, Rev. Mod. Phys. **78**, 641 (2006).
[3] F. Melo, P. B. Umbanhowar, and H. L. Swinney, Phys. Rev. Lett. **75**, 3838 (1995).
[4] A. Prevost, P. Melby, D. A. Egolf, and J. S. Urbach, Phys. Rev. E **70**, 050301(R) (2004).

[5] J. S. Olafsen and J. S. Urbach, Phys. Rev. Lett. **81**, 4369 (1998).
[6] J. S. Olafsen and J. S. Urbach, Phys. Rev. Lett. **95**, 098002 (2005).
[7] O. Dauchot, G. Marty, and G. Biroli, Phys. Rev. Lett. **95**, 265701 (2005).
[8] P. M. Reis, R. A. Ingale, and M. D. Shattuck, Phys. Rev. Lett. **98**, 188301 (2007).
[9] A. Prevost, D. A. Egolf, and J. S. Urbach, Phys. Rev. Lett. **89**, 084301 (2002).
[10] P. M. Reis, R. A. Ingale, and M. D. Shattuck, Phys. Rev. E **75**, 051311 (2007).
[11] T. P. C. van Noije and M. H. Ernst, Granular Matter **1**, 57 (1998).
[12] G. W. Baxter and J. S. Olafsen, Nature (London) **425**, 680 (2003).
[13] P. Cundall and O. Strack, Geotechnique **29**, 47 (1979).
[14] G. W. Baxter and J. S. Olafsen, Phys. Rev. Lett. **99**, 028001 (2007).
[15] K. Combs, J. S. Olafsen, A. Burdeau, and P. Viot, Phys. Rev. E **78**, 042301 (2008).
[16] A. Burdeau and P. Viot, Phys. Rev. E **78**, 041305 (2008).
[17] H. Gomart, J. Talbot, and P. Viot, Phys. Rev. E **71**, 051306 (2005).
[18] G. Costantini, U. Marini Bettolo Marconi, and A. Puglisi, Phys. Rev. E **75**, 061124 (2007).
[19] B. Cleuren and R. Eichhorn, J. Stat. Mech.: Theory Exp. (2008) P10011.